Theory-Based Improvements of Continuous Polymer Fractionation Demonstrated for Poly(carbonate)

K. WEINMANN,[1] B. A. WOLF,[1,*] M. T. RÄTZSCH,[2] and L. TSCHERSICH[2,†]

[1]Institut für Physikalische Chemie der Universität Mainz and SFB 262, Jakob-Welder Weg 13, DW 6500 Mainz, Germany, and [2]Institut für Physikalische Chemie der Technischen Hochschule Merseburg, Otto Nuschke Straße 42, DO4200 Merseburg, Germany

SYNOPSIS

For the first time, a quantitative theoretical analysis (liquid/liquid phase equilibria treated by means of the continuous thermodynamics) of the operating characteristics of continuous polymer fractionation (CPF) was performed. The results of these calculations were compared with data published for CPF of polyethylene. It turned out that the efficiency of the conventional CPF corresponds to approximately two theoretical plates only. For this reason, several improvements, suggested by theoretical considerations, were realized experimentally, for which purpose the system dichloromethane/diethylene glycol/bisphenol-A polycarbonate was chosen. The pulsating sieve-bottom column was replaced by a nonpulsating column filled with glass beads. In this manner, the number of theoretical plates could be raised considerably. A further improvement of the fractionation efficiency results from the reflux of part of the polymer contained in the sol phase. *In praxi,* this situation was realized by putting a condensor on top of the column and introducing the feed somewhere near its upper third. After predictive calculations and orienting experiments, 125 g of a polycarbonate with M_w = 29 kg/mol and a nonuniformity U = 1.3 were fractionated in four consecutive CPF runs (where the gels were directly used as feed for the next step) into five fractions of approximately equal weight. Except for the lowest-molecular-weight fraction, one obtains nonuniformities on the order of 0.1.

INTRODUCTION

Continuous polymer fractionation (CPF) was developed to produce large amounts of material with narrow molecular weight distribution.[1-3] It consists of a countercurrent extraction that functions in the following way: A comparatively concentrated solution of the polymer in a given solvent (the feed) is introduced into a column on one end and the same solvent but free of polymer (extracting agent) on the other. Both phases are homogeneous as they enter the column, but demix inside such that the molecules of different mass distribute between the two phases. The high-molecular-weight material remains in the phase resulting from the feed and leaves the column as the gel phase, whereas the low-molecular-weight material is extracted and yields the sol phase. Normally, one uses mixed solvents, but CPF can also be operated with one-component theta solvents.[3] So far, CPF was operated with a pulsed sieve-bottom column.

The advantages and drawbacks of this method, as compared with conventional fractionation procedures, were recently discussed in a review article.[4] A critical assessment of the efficiency that could be realized with CPF so far demonstrates that it remains far below expectation in view of the chromatographic nature of this method.

We therefore attempted a theoretical modeling of CPF to obtain clues concerning possibilities for improvement. The basis for such calculations has recently been laid by the simulation of Baker–Williams fractionation by means of continuous thermodynamics.[5] Taking account for the polymolecularity of the solute by direct use of the continuous

* To whom correspondence should be addressed.

† DAAD Fellow at the University of Mainz from September 1989–February 90.

Journal of Applied Polymer Science, Vol. 45, 1265–1279 (1992)
 CCC 0021-8995/92/071265-15$04.00

distribution functions in the thermodynamic equations leads to clearly arranged and lucid expressions particularly suited to computer calculations.

In the present contribution, a similar treatment will be performed for CPF and compared with published experimental results. Furthermore, we aim to realize the improvements suggested by this theoretical study using polycarbonate.

THEORY OF COLUMN FRACTIONATION

The theoretical basis of the polymer distribution between two phases is formed by the thermodynamics of liquid/liquid (1/1) equilibria of polymer solutions. Detailed treatments by continuous thermodynamics[6,7] and the application to successive polymer fractionation[8] and to the Baker–Williams process[5] were presented earlier. For this reason, only a brief outline is given here. To keep experimental information required for the theoretical calculations as low as possible, mixed solvents are treated as one component. This procedure can be justified by the fact that our interest is primarily in the partition of the macromolecules and not in that of the components of a mixed solvent.

Fractionation Equilibria

The number of segments r of a polymer molecule of mass M is defined by the molar mass of a segment, M_{seg}, according to

$$r = M/M_{seg} \tag{1}$$

where r_A is the number of segments of a solvent molecule. The weight fraction of molecules with the number of segments r is given by the segment molar distribution function $W(r)$; $W(r)dr$ equals the segment fraction of all polymer species with segment numbers between r and $r + dr$. If r_0 is the lowest and r^0 the largest segment number to be considered, the normalization condition reads

$$\int W(r)dr = 1 \quad \text{where} \quad \int \text{ means } \int_{r_0}^{r^0} \tag{2}$$

The number average of segments per macromolecule r_n is given by

$$1/r_n = \int [W(r)/r]dr \tag{3}$$

The average $\langle r \rangle$ of the entire material contained in one phase can be calculated according to

$$1/\langle r \rangle = (1 - \Psi)/r_A + \Psi/r_n \tag{4}$$

where Ψ means the overall segment fraction of the polymer.

The equations describing the phase equilibrium are obtained by combining the equilibrium conditions with the material balances. Continuous thermodynamics of the 1/1 equilibrium yields the following simple expressions that relate the distribution functions of the polymers in the two coexisting phases, designated by ′ and ″, with that of the entire polymeric material prior to phase separation (superscript zero).

$$\Psi' W'(r) = \Psi^0 W^0(r)[1 - K(r)]/[1 - \Phi] \tag{5}$$

$$\Psi'' W''(r) = \Psi^0 W^0(r) K(r)/\Phi \tag{6}$$

Φ gives the fraction of all segments (solvent included) present in the starting solution that forms phase ″ and K is the degree of precipitation as a function of the number of segments r.

$$K(r) = \Phi[\Psi'' W''(r)]/[\Psi^0 W^0(r)] = \Phi/[\Phi + (1 - \Phi)\exp(-r\rho)] \tag{7}$$

where ρ is given by the average r values and γ, the segment molar activity coefficients.

$$\rho = (1/\langle r'' \rangle) - (1/\langle r' \rangle) + \ln \gamma' - \ln \gamma'' \tag{8}$$

Equations (5) and (6) provide directly[8] the unknown distribution functions $W'(r)$ and $W''(r)$ if $W^0(r)$ and Ψ^0 are given and Ψ'', $\langle r'' \rangle$, and Φ calculated from the following set of equations. These relations, referring to the gel phase, result from a combination of equilibrium conditions and material balances. The other required quantities can be easily calculated,[8]

$$1 - \Psi'' = (1 - \Psi^0)/[\Phi + (1 - \Phi)\exp(-r_A \rho_A)] \tag{9}$$

$$\Psi'' = \int \Psi^0 W^0(r) K(r)/\Phi dr \tag{10}$$

$$1/\langle r'' \rangle = (1 - \Psi'')/r_A + \int \Psi^0 W^0(r) K(r)/(\Phi r)dr \tag{11}$$

where ρ_A is given by

$$\rho_A = (1/\langle r'' \rangle) - (1/\langle r' \rangle) + \ln \gamma'_A - \ln \gamma''_A \quad (12)$$

In case the γ values are independent of the molecular weight distribution, one of the above equations can be eliminated by substituting for $\langle r'' \rangle$.

For the actual calculation, expressions for γ_A and γ are required. Per definition, the following relation holds true for the differential quantity

$$RT \ln \gamma_A = \Delta G_A^R \quad (13)$$

in which ΔG_A^R is the residual *segment* molar Gibbs energy of the solvent. The integral residual segment molar Gibbs energy of mixing is related to the (integral) Flory–Huggins interaction parameter g by

$$\Delta G^R = RT[(1 - \Psi)/r_A]\Psi g \quad (14)$$

Normally, g depends on composition. In many cases, the experimental data can be represented by

$$g = g_0(1 + p\Psi) \quad (15)$$

where g_0 and p are normally varying with temperature. From the above equations, one obtains

$$r_A RT \ln \gamma_A = \Psi^2 g_0[1 - (1 - 2\Psi)p] \quad (16)$$

and

$$r_A RT \ln \gamma = (1 - \Psi)^2 g_0(1 + 2\Psi p) \quad (17)$$

For further calculations, two procedures leading to practically identical results were tested:

1. $M_{seg} = M_A$ (i.e., $\Psi = w_{pol}$, the weight fraction of polymer) and p is chosen such as to describe the experimental findings.
2. $(M_{seg})_{pol} \neq (M_{seg})_A$ and the latter quantity set equal to M_A so that $r_A = 1$; for concentration-independent g ($p = 0$), M_{seg} is adjusted. In this case, Ψ depends on w_{pol} according to

$$\Psi^{-1} = M_{seg}/M_A(w_{pol}^{-1} - 1) + 1 \quad (18)$$

Procedure 2 is simpler in nature and was therefore adopted for the subsequent calculations. The underlying assumption of the segmental masses of solvent and of solute being different does not appear unreasonable. $(M_{seg})_{pol} \neq (M_{seg})_A$ is even a necessary consequence of lattice theories (in which the site volume is kept constant) as soon as the densities of the components differ. Further effects that can be incorporated into the segmental masses by proper adjustment are differences in the molecular shapes and flexibilities.

The data resulting from procedure 2 are in the following discussed for the system diphenyl ether/poly(ethylene) (DPE/PE) (cf. Fig. 2). $M_{DPE} = M_A = 170$ g/mol yields a segmental volume of 158 cm^3/mol; from the adjustment of equilibrium fractionation data, one obtains $(M_{seg})_{PE} = 115$ g/mol, which would lead to a segmental volume for the polymer of 119 cm^3/mol (instead of 158). In view of the fact that DPE is comparatively bulky in contrast to PE, which is thin and flexible, the remaining difference does not appear unreasonable.

For a good analytical representation of experimental results, it is furthermore necessary to consider an additional effect, namely, the leveling off of fractionation efficiency at high molecular weights. For thermodynamic reasons, the partition coefficient should become zero in the limit of infinitely long chains

$$\lim_{r \to \infty} [\Psi' W'(r)]/[\Psi'' W''(r)] = 0 \quad (19)$$

Experimental results, however, indicate that this quantity remains finite.

One plausible explanation for that observation could lie in the specific way in which the molecules forming the gel phase are transferred into it from the starting (subcritical) solution upon the gradual deterioration of solvent power. In the initial state, the number of nuclei is large enough to exclude any supersaturation. In the final stages, during which the rest of the high-molecular-weight material has to be incorporated into the gel phase, this is not true any more. The less concentrated phase has meanwhile become so dilute and free of nuclei that supersaturation can easily take place. This situation remains almost inconsequential for the shorter chains since the minute cut-off of transport does not measurably change the equilibrium partition coefficient. This is, however, no longer true for the longer chains since this supersaturation effect can even double the minute amount present under equilibrium conditions (and therefore increase the nonuniformity of the sol fraction noteworthy). To take account for this fact, eq. (7) was modified in the following way

$$K(r) = \Phi[\Psi'' W''(r)]/[\Psi^0 W^0(r)] = \Phi/\{\Phi + (1 - \Phi)[\exp(-r_\rho) + \xi]\} \quad (20)$$

and ξ treated as an adjustable parameter.

Modeling of CPF

The CPF process is represented by a column consisting of a certain number of theoretical plates where each of these plates corresponds to a 1/1 phase equilibrium. Figure 1 shows the model used for the subsequent calculations.

For conventional CPF, where the feed (FD) is introduced on top, the calculation of stationary states starts ($j = 0$) with the entire column filled with extracting agent (EA). For the first set of equilibria ($j = 1$), a certain amount of FD, determined by the chosen working conditions of CPF, is introduced at m_{FD}. After the equilibrium has been calculated for this plate, phase $''$ is transferred downward into the next theoretical plate (filled with EA) and the new equilibrium on plate $m_{FD} + 1$ is determined. This procedure is repeated until phase $''$ leaves the column as the first (nonstationary) gel phase at m_{max}. In preparation of the next step of calculation ($j = 2$), all phases $'$ are shifted by one plate upward [i.e., from m to $m - 1$ so that the first (nonstationary) sol phase leaves the column at m_{FD}]; furthermore, plate m_{max} is again filled with pure EA. After the addition of another portion of FD, the determination of the next set of equilibria ($j = 2$) proceeds as described for $j = 1$. This treatment is repeated until the stationary state is reached, which means that the results for j and $j - 1$ do no longer change systematically.

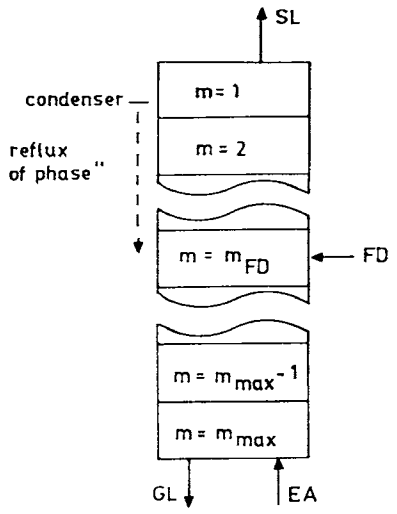

Figure 1 Representation of CPF used in the theoretical treatment for which it is assumed that the phase rich in polymer is the denser one; m numbers the theoretical plate under consideration. The feed (FD) enters the column at $m = m_{FD}$ and the extraction agent (EA) at $m = m_{max}$. The polymer fractions leave the column as gel (GL) at $m = m_{max}$ and, in the case of conventional CPF, as sol (SL) at $m = m_{FD}$. For improved CPF (discussed in more detail in the section dealing with the improvements suggested by theory), a condenser is introduced on top of the column to reflux phase $''$; with this modification, the SL leaves at $m = 1$.

The mass balance for the polymer transfer is formulated in terms of $w(r)$, their extensive segment molar distributions obtained by multiplying $W(r)$ with the overall amount of polymer segments present in a given system. For the transfer between neighboring phases, the following relation can be formulated

$$w'_{m+1,j-1}(r) + w''_{m-1,j}(r) = w^0_{m,j}(r) \qquad (21)$$

For $j = 1$, the first term becomes zero and for $m = m_{FD}$ the additional term $w_j^{FD}(r)$ has to be added on the left side of the equation; for $m = m_{max}$ the first and for $m = 1$ the second term vanish. In the case of conventional CPF, m_{FD} is equal to unity. For the mass balance for the subdivision of the polymer among the phases coexisting on one theoretical plate, the corresponding equation reads

$$w^0_{m,j}(r) = [w'(r) + w''(r)]_{m,j} \qquad (22)$$

In the calculation outlined above, the number of segments contained in a theoretical plate changes with j within the nonstationary phase. For this reason, a quantity ϵ is introduced as the ratio of the overall amount of segments present in plate m during step j and during step zero. From the material balance between adjacent theoretical plates, one obtains the following relation

$$\epsilon_{m,j} = [\epsilon(1 - \Phi)]_{m+1,j-1} + (\epsilon\Phi)_{m-1,j} \qquad (23)$$

with the limiting condition $\epsilon_{m,0} = 0$ for $m = 1$ up to $m = m_{FD} - 1$ (improved CPF) and $\epsilon_{m,0} = 1$ for $m = m_{FD}$ to $m = m_{max}$ and for $m = m_{FD}$ the extra term ϵ^{FD} (which is determined by the amount of segments added with the feed, normalized to the amount of EA present on this plate for $j = 0$) has to be added on the right side of the equation. For $m = m_{max}$ and $j > 0$, the first term becomes unity and for $m = 1$ the second vanishes. To obtain the material balances for the polymer, eqs. (21) and (22), in terms of the normalized distributions $W(r)$, one divides these relations by the total amount of segments in a plate at $j = 0$. This leads to

$$[\epsilon(1 - \Phi)\Psi'W'(r)]_{m+1,j-1} + [\epsilon\Phi\Psi''W''(r)]_{m-1,j} = [\epsilon\Psi^0W^0(r)]_{m,j} \qquad (24)$$

where the special cases discussed in the context of eq. (21) apply analogously, and to

$$[\Psi^0 W^0(r)]_{m,j} = [(1-\Phi)\Psi' W'(r) + \Phi\Psi'' W''(r)]_{m,j} \quad (25)$$

The actual model calculations are performed in the following way: For $j = 1$ and $m = m_{FD}$, $\Psi^0 W^0(r)$ is given by the molecular weight distribution of the polymer to be fractionated and its concentration on this plate (in this special situation equal to the working point WP of the CPF). Ψ^0, w_{wp}, and $\epsilon^{FD}\Psi^{FD}$ are interrelated by eqs. (18), (23), and (24). After a suitable choice of g (normally held constant for conventional CPF) the phase equilibrium for this theoretical plate can be calculated by determining the characteristic parameters Ψ'', Φ, and $\langle r'' \rangle$ from eqs. (9)-(11).

Next, phase $''$ is transferred to the plate $m_{FD} + 1$ where for $j = 1$ it constitutes the only source of polymer. The ϵ value required in eq. (24) can be obtained from eq. (23) where the first term on the right equals to unity and the second is known from the previous calculation. After that, $\Psi^0 W^0(r)$ for $m = m_{FD} + 1$ and $j = 1$ is accessible from eq. (24), where the first term on the left is zero and the second known again. Now, all data required for the calculation of the equilibrium on plate $m = m_{FD} + 1$ and $j = 1$ are available so the procedure practiced with $m = m_{FD}$ can be repeated. As described in the beginning of this section, the stationary state is approached by a stepwise calculation of the compositions of the coexisting phases, where the information concerning all previous states is required in the actual calculation.

APPLICATION OF THEORY

This section deals with the application of the theoretical equations for the simulation of CPF, given in the previous section, to published experimental data. The system DPE/PE[3] was chosen for that purpose since problems with mixed solvents, so far not introduced explicitly in the theory, are avoided. Furthermore, a critical assessment of this evaluation in view of improvements of the CPF process will be given.

Evaluation of Published CPF Results

Numerical calculations were performed on a home computer (Atari 1040 ST) using FORTRAN 77. The integrals of eqs. (10) and (11) must be solved numerically. If $W(r)$ is given analytically, one may use an integrating routine. In the present case, information concerning the molecular weight distributions is available in the form of gel permeation chromatography (GPC) data. For that reason, it is preferable to treat the integration as a summation. However, the number of data points has to be sufficiently large and well chosen (e.g., equal distance on a logarithmic scale) to obtain the same results as with the (preciser) numerical integration. Unfortunately, there does not exist a general rule concerning the required number of data, but by means of model calculation with both methods it was found out that a number of approximately 100 is normally sufficient. To simulate one stationary state of CPF as described, the necessary computer time increases with the number of theoretical plates from a few minutes ($m < 4$) up to approximately 1 h ($m \approx 10$).

To determine the parameters necessary for the simulation of the CPF of PE with DPE as solvent, the corresponding data for (discontinuous) fractionation equilibria are used. From Breitenbach-Wolf (B-W) plots[9] $\{\log[w'(M)/w''(M)]$ vs. M, cf. Fig. 2$\}$, one can read $\log \xi$ [cf. eq. (20)] as the distance of the asymptote from the intercept with the ordinate; the slope of the linear part of this plot (a measure of fractionation efficiency for a given size of the fractions) is according to theory proportional to ρ [eq. (8)]. It can be changed, as discussed in the section dealing with fractionation equilibria, in two ways. For the present calculation, M_{seg} was altered and the interaction parameters g treated as concentration independent. In practice, one starts from the experimentally determined ratio of the polymer amounts in the two fractions, chooses a reasonable value for M_{seg}, and calculates g. This procedure is repeated varying M_{seg} until the slope of the theoretical B-W plots coincides with the experimental ones.

Figure 2 gives an example for the above evaluation. For the two concentrations indicated in the graph, the experimental results (measuring points) are compared with the theoretical calculations (lines); the values of the parameters used are given in the legend. The agreement is very satisfactory in view of the different approximation and the comparatively simple eq. (20). The fact that the equilibrium fractionation can be represented very accurately allows a trustworthy simulation of the CPF.

Before that, a few words concerning the sensitivity of the results to the values chosen for g, ξ, and M_{seg} appear appropriate. Model calculations have shown, as expected, that a variation of g on the order

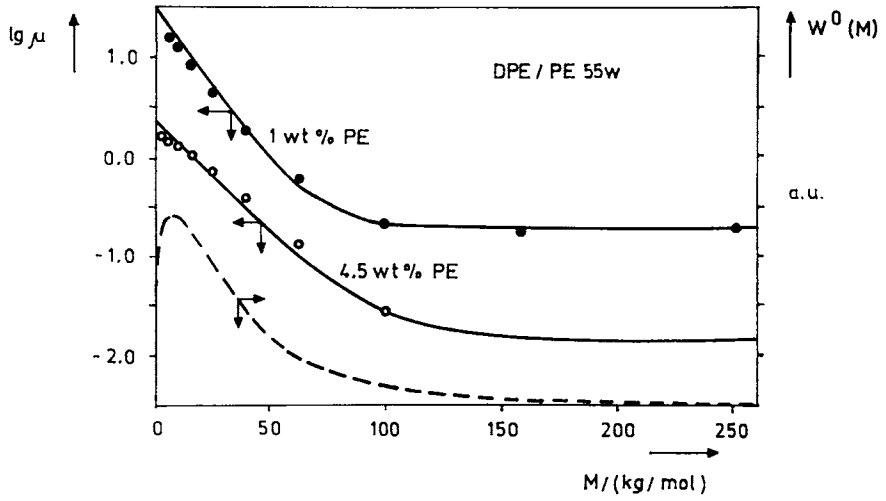

Figure 2 B–W plot [logarithm of the ratio μ of the masses of polymer species with molecular weight M in the sol and in the gel phase as a function of M, where $\mu = w'(M)/w''(M)$] for two solutions of poly(ethylene) in diphenyl ether of the indicated concentration at 133°C. Points represent a selection of measured data[3]; the result of the theoretical calculation is given by the solid lines, where the following values were used: $\xi = 6 \cdot 10^{-3}$, $M_{seg} = 115$ g/mol (as compared with 170 g/mol for the solvent), and $g = 0.577$. To demonstrate which part of the B–W plot is really important for fractionation, the molecular weight distribution of the original sample is also shown (broken line).

of 1% changes the ratio of the polymer masses in the coexisting phases quite drastically, namely, up to ca. 15%. The values of the parameter ξ, on the other hand, are less influential since they only correct for the decreasing fractionation efficiency at high molecular weights. If ξ is set to zero, the nonuniformity of the sol fraction decreases by approximately 25% and that of the gel changes correspondingly. The accuracy of the experimental data allows ξ to be fixed with an uncertainty of ca. 10%. Finally, a variation of M_{seg} by 5% leads to a change in the U values of the fractions by approximately the same percentage. However, it has to be borne in mind that M_{seg} can differ substantially from M_A.

To treat an actual CPF experiment (same system, same T) theoretically, one uses the ξ and M_{seg} values determined from equilibrium experiments as described above; in principal, one could also maintain the g value in the determination of the number of theoretical plates. This, however, would lead to difficulties because the m values are only integers in the present theoretical approach, whereas the experimentally realized numbers of theoretical plates m_{exp} can also be nonintegers. Since the size of the two CPF fractions depends on both, m and g, the theory can only reproduce the experiments with respect to the size *and* to the distribution of the fractions as long as m_{exp} is by incidence an integer. To overcome this difficulty, one chooses the integer m giving the best agreement with reality and modifies g slightly so that the size of the fractions is exactly reproduced and a comparison of calculated and measured molecular weight distributions becomes possible. The results shown in Figure 3 for an actual CPF experiment were obtained with $m = 2$ as just outlined.

The fact that only two theoretical plates were reached with conventional CPF (as demonstrated in the above diagram) is generally observed and very unsatisfactory in view of the chromatographic nature of this separation process. For that reason, improvements one could find out on the basis of the present theoretical modeling of CPF will be analyzed in the next section.

Improvements Suggested by Theory

There are several conceivable explanations for this finding. One possibility would be that the velocity of exchange of matter over the phase boundary is too low either in the later stages of the process or during the entire extraction. Another hypothesis concerns unwanted mixing of the matrix phase of CPF by backflow due to the turbulences associated with pulsation; it causes an obstruction of the countercurrent, i.e., a deterioration of separation. As shall

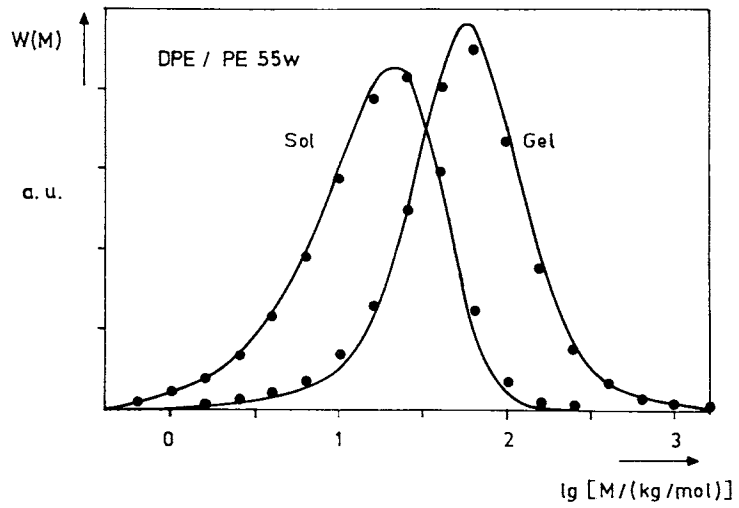

Figure 3 Comparison of measured (points) and calculated molecular weight distributions (lines) for the first fractions (cf. Fig. 10 of ref. 3) of poly(ethylene) obtained with CPF (equal amounts of polymer in the sol and in the gel phase). The calculation was performed for two theoretical plates and the following parameters: $\xi = 6 \cdot 10^{-3}$, $M_{seg} = 115$ g/mol, and $g = 0.573$.

be demonstrated in the discussion, it is this idea that proves to be decisive.

A further important aspect that could explain the unsatisfactory fractionation with conventional CPF lies in the following situation: The polymer contained in the feed enters at a point where it contacts the sol phase, depleted of higher-molecular-weight material, just before it leaves the column. For this reason, the separation cannot proceed to a point where the sol is practically free of long chains. To eliminate this drawback, one could think of a procedure working analogously to rectification. This means that the feed should be introduced sufficiently far from the sol exit and part of the polymer contained in the sol phase of conventional CPF should be refluxed in the dispersed phase. In practice, this can easily be done by inserting at the sol exit of the column either a condenser (low-temperature demixing) or a heater (high-temperature demixing).

Quantitative calculations on the basis of the equations formulated in the theoretical section were now performed to see whether the modified operation of CPF would really improve the efficiency of fractionation. In the stepwise calculation of the approach of stationary states, one starts as described for conventional CPF, i.e., m is varied from $m = m_{FD}$ to $m = m_{max}$; as soon as the polymer has reached the condenser ($m = 1$), the procedure is applied $m = 1$ to $m = m_{max}$.

To obtain results that can be directly compared with experimental data, these calculations were performed for the system dichloromethane/diethylene glycol/poly(carbonate) ($M_w = 29$ kg/mol) (DCM/DEG/PC 29w). The working point w_{WP} (weight fraction of polymer in the entire column, calculated from the fluxes of feed and extracting agent) was in all cases kept constant at 0.02 and the interaction parameter g selected such that the starting polymer is subdivided in two fractions of equal weight. It was calculated how the molecular nonuniformity of the fractions depends on the number of theoretical plates and the position of the feed entrance.

Figure 4(a) shows the results with respect to the variation of the number of theoretical plates in the case of conventional CPF and in the case of the feed entrance in the middle of the column.

The efficiency is, as expected, considerably higher for larger values of m_{max} if part of the polymer is refluxed. However, at lower numbers of theoretical plates the separation becomes even worse with the new vesion of CPF. This can be explained by the following consideration: Since polymeric material is exclusively extracted from the feed between its entrance and the exit of the gel, the thermodynamic quality of the solvent that is necessary to guarantee a one by one subdivision of the material into fractions increases almost exponentially as the distance between these two locations becomes smaller. This leads to less dissimilar coexisting phases and eventually to a deterioration of fractionation efficiency due to a smaller chain length dependence of the partition coefficient for the different homologues.

The question where the feed should be entered

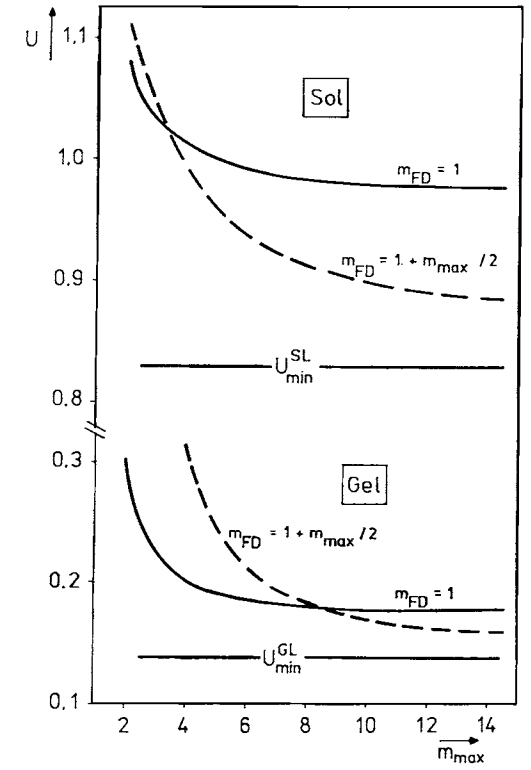

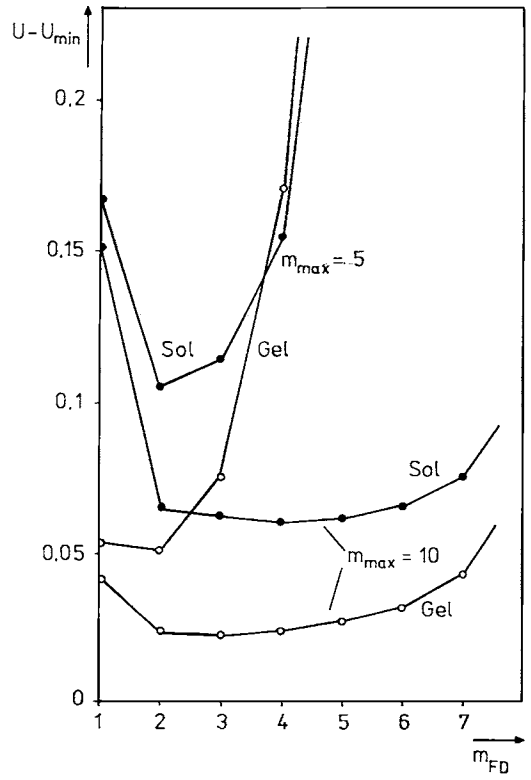

Figure 4 Comparison of the nonuniformities U calculated for the sol and gel fractions, respectively, as a function of the number m_{max} of theoretical plates of the column and the position of the feed entrance. The working point of the polymer was set to 0.02 and the interaction parameter g taken to be constant within the entire column except for the condenser (equal to one theoretical plate), for which an interaction parameter higher by 0.013 was chosen (in reality, corresponding to a decrease in temperature of approximately 20°C). Now, the values of g were selected such that the polymer is subdivided into fractions of equal weight. The following parameters, representing the system DCM/DEG/PC 29w, were used: $M_{seg} = 70$ g/mol, $M_{mixed\ solvent} = 88.5$ g/mol, $\xi = 2 \cdot 10^{-3}$. U_{min} is the molecular nonuniformity one would obtain if all chains below a certain characteristic molar mass would be found in the sol and all above it in the gel fraction. (a), U^{SL} and U^{GL} as a function of m_{max} for conventional CPF (full line, feed entrance at the end of the column) and for one example of improved CPF (broken line, feed entrance in the middle of the column); (b), dependence of $U - U_{min}$ on the location of the feed entrance for 10 and 5 theoretical plates, respectively; $m_{FD} = 1$ corresponds to conventional CPF.

into the column with improved CPF cannot be answered generally but depends on the total number of theoretical plates available, as is demonstrated in Figure 4(b). As a rule of thumb, one can state that for $m_{max} \geq 5$ the part of the column between feed entrance and condenser should be approximately one third of the total length.

The present theoretical calculations can also supply some guidelines concerning the best strategy for the successive application of CPF. So far, the polymer was normally subdivided in approximately equal fractions in each step. The simulation of different procedures demonstrates, however, that it is considerably better to extract small amounts of low-molecular-weight material in the different individual CPF runs. This not only leads to higher fractionation efficiencies as a result of the positioning of the working point deeper inside of the solubility gap. It also has practical advantages since the gel phases can directly be used as feeds for subsequent CPF runs and fluctuations in the working conditions are of much lesser consequence. Furthermore, and this is of great practical importance, one saves considerable amounts of solvent by this procedure since one final fraction is obtained in each step.

EXPERIMENTAL REALIZATION AND IMPROVEMENTS WITH POLY(CARBONATE)

Features of Improved CPF

Apparatus

Three principal alterations were made with respect to the device used so far.[2] The pulsating sieve-bottom

column was replaced by a column of 2 m length and 3 cm diameter and entirely filled with packing material (glass beads of normally 4 and in one experiment of 8 mm diameter). For the present experiments (low-temperature demixing, polymer density larger than that of the mixed solvent), a condenser of high performance, through which the leaving sol has to pass, was inserted on top of that column. The feed is introduced 50 cm below the condenser. It turns out essential to apply packing material between the condenser and the feed entrance to prevent convective mixing outside of the cooling zone.

Procedure

Following the theoretical suggestion that the sol fractions should be cut out of the molecular weight distribution of the initial polymer successively, it was planned to subdivide the material into five fractions of approximately equal weight, i.e., to perform four consecutive CPF runs. To this end, one keeps the operating temperature constant at ambient conditions and improves the thermodynamic quality of the extracting agent appropriately in each step. The temperature of the condenser is selected such that approximately one third of the polymer extracted from the feed refluxes. For practical purposes, it has turned out helpful to fill the column to the feed entrance with pure extracting agent before adding feed.

Materials

Polymer

Bisphenol-A [poly(4,4'-isopropyliden-diphenylencarbonat)], a technical sample of Makrolon, was kindly supplied by Bayer AG (Leverkusen, FRG). M_w = 29 kg/mol and U = 1.3.

Solvents

The organic liquids used and some of their physical properties that are of importance in the context of CPF are presented in Table I.

Auxiliary Methods

Cloud Points

To determine the limits of complete miscibility of the polymer and the mixed solvents, cloud points were measured visually at constant temperature by titrating solutions of the polymer with the precipitant.

Phase Equilibria

Data concerning the equilibrium demixing behavior, required for the theoretical modeling of CPF, were obtained by cooling homogeneous solutions slowly to the end temperature. Samples of the coexisting phases were taken by means of a syringe.

GPC

The system consists of μ-Styrogel columns with 10^3, 10^5, and 10^6 Å pore diameter. Freshly distilled tetrahydrofuran (THF) was used as solvent, and the volume of the injected polymer solutions (approx. 2×10^{-3} g polymer/cm^3) was 50 μL. The flow rate amounted to 1 cm^3/min. The composition of the effluent stream is detected by means of a differential refractometer from Showadenko and by a UV detector from Knauer at 254 nm.

Molecular weights were calculated from the data obtained with polystyrene standards by means of the universal calibration.[10] It was checked by means of polycarbonate standards (Polymer Standards Service, Mainz, FRG) that this procedure is permissible. Further evaluation with respect to the different molecular weight averages and nonuniformities was performed using the program "Gelchromatographie" from EQUTOL-PSS (Mainz, FRG). For analysis of the polymers contained in the coexisting phases, solutions were diluted appropriately with THF, containing a small amount of toluene as internal standard, freed of dust, and injected as soon as homogenous without further delay to avoid degradation of the polycarbonate.

Table I List of Solvents

Solvent	Abbreviation	Producer	Purity
Tetrahydrofuran	THF	Merck	p.a.
Dichloromethane	DCM	Bayer	Technical grade
2-Propanol	2-POH	Bayer	Technical grade
Methanol	MeOH	Bayer	Technical grade
Diethylene glycol	DEG	Merck-Schuchardt	For synthesis

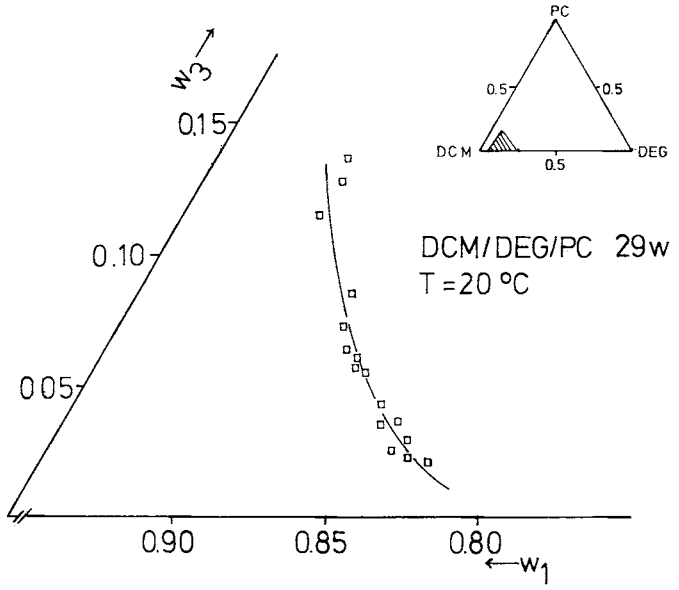

Figure 5 Cloud-point curve of the system DCM/DEG/PC 29w at 20°C in the region that interests in the context of CPF experiments.

Conditions for the Different CPF Runs

The choice of suitable combinations of solvent/nonsolvent pairs turned out to be problematic because of degradation and/or crystallization of the polymer. Detailed measurements were performed with the following three mixed solvents: DCM/MeOH (I), DCM/2-POH (II), and DCM/DEG (III). Only III turned out to be good enough for the CPF; with I, the polymer is particularly susceptible to degradation (transesterification) and with II the liquid/liquid phase separation is only metastable as compared with liquid/solid. Even with III, however, special care must be applied to dry all liquids and to neutralize DCM quantitatively. To this end, DCM was stored over K_2CO_3 and freshly distilled before use to get rid of traces of solid carbonate, which also turned out to catalyze degradation. The cloud-point curve for solutions of PC 29w in the above-mixed solvent III is shown in Figure 5 for 20°C.

How the different CPF runs were performed can be seen from Table II, in which the data of all essential experiments are collected.

RESULTS AND DISCUSSION

CPF Experiments

Test runs with the apparatus of conventional CPF (pulsated sieve-bottom column,[2] experiment A of Table II) and with a modified nonpulsated version,

Table II Experimental Data of the Different CPF Runs

CPF Run	FD (w_2|w_3)	EA (w_2)	ϑ/°C (column|condenser)	w_{WP}	Fluxes/g h^{-1} (FD|EA)
A[a]	0.13|0.05	0.220	23|—	0.025	320|308
B[b]	0.11|0.08	0.200	23|—	0.018	85|300
C1[c]	0.08|0.15	0.220	21|−3	0.013	25|260
C2	Gel of C1	0.210	23|+1	0.015	20|200
C3	Gel of C2	0.198	25|+5	0.012	15|200
C4	Gel of C3	0.190	25|+12	0.017	23|190
D[d]	0.08|0.15	0.190	21|+11	0.032	78|292

[a] Conventional CPF using the apparatus of ref. 2.
[b] Same apparatus without pulsation, packed with glass beads of 4–5 mm diameter.
[c] Improved CPF, glass beads of 4 mm diameter.
[d] Improved CPF, glass beads of 8 mm diameter.

in which the column is filled with glass beads of 4- to 5-mm diameter (experiment B), have proven the hypothesis that the poor efficiency of A is primarily caused by backflow phenomena. In case A, a weight fraction of 0.59 of the starting polymer is found in the gel that possesses a nonuniformity of 0.46, and in case B the corresponding values read 0.57 and 0.32. An analysis of these results in terms of theoretical plates yields a number only slightly larger than unity for A but approximately 2 for B.

With the new apparatus for the improved CPF described in the experimental section, a series of experiments was performed (runs C in Table II). Its primary goal consisted in the successive subdivision of the starting material into five fractions of approximately equal size. The results of these runs are shown in Figure 6. Except for the first fraction, where the molecular weight distribution of the starting material does not permit a low U value if it has to contain 20% of the material, the results are very satisfactory. The capacity lies typically on the order of 3–4 g polymer per hour with the present apparatus. This fact appears disappointing at first if one compares it with the considerably higher loading of the conventional CPF. It must, however, be borne in mind that due to the presence of the filling material only a small portion of the column is available and that the working point cannot be raised without limits: If the flux of feed exceeds a certain critical value, this phase will be dammed back.

To check whether larger interstitial volumes can help raise the working point, one CPF experiment was performed with larger diameters of the glass spheres, namely, 8-mm diameters instead of 4 (CPF run D in Table II). Indeed, it was possible to elevate the working point from 1.5 wt % polymer to 3.2; in spite of the higher polymer concentration, the fractionation quality was only slightly worse than in the case of experiment C1: 43 wt % polymer was extracted in the sol phase and the gel fraction obtained had a nonuniformity of 0.32. These data correspond to a slightly larger number of theoretical plates for CPF run D as compared with C1. The evaluation of the present data with respect to the fluxes yields approximately 12 g polymer per hour, i.e., an increase in the capacity by a factor of 3 to 4. Taking the space filling of the glass beads into account, this result is comparable with that of conventional CPF. Experiment D shows one way how improved CPF can be further optimized.

A more direct graphical assessment of the effi-

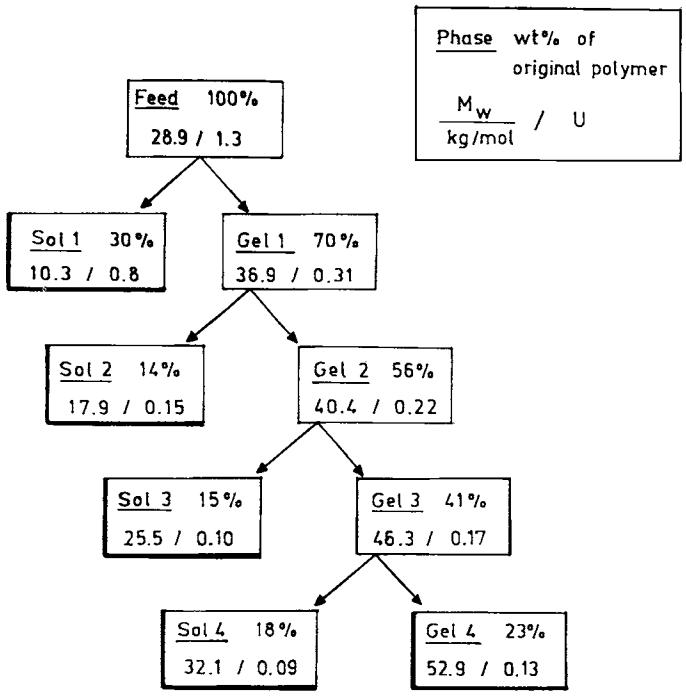

Figure 6 Schematic representation of results obtained with a series of consecutive CPF runs using improved CPF; the five final fractions are underscored. The conditions can be seen in Table II under the letter C.

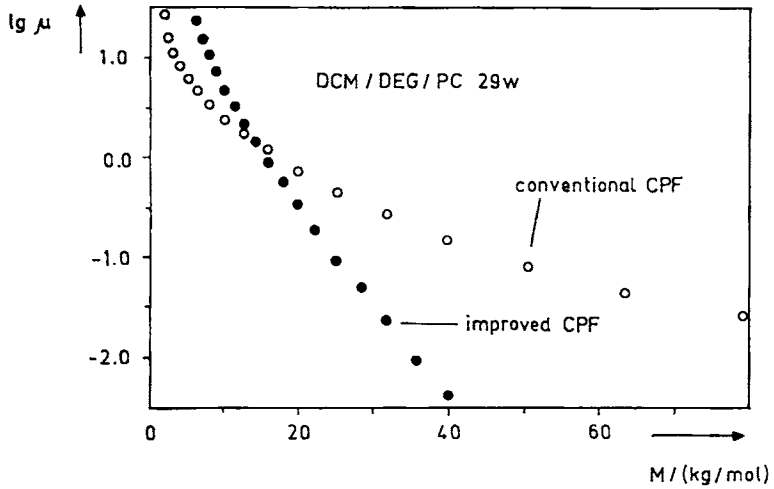

Figure 7 B–W plot for CPF runs A and C1 of Table II. Points represent a selection of measured data.

ciency of the fractionations achieved with conventional and improved CPF, respectively, is offered by B–W plots. Such an evaluation is shown in Figure 7 for experiments A (conventional) and C1 (improved); although the subdivision of the polymer onto the fractions and the working points of the two CPF runs differ to some extent, the larger slope for C1 can beyond doubt be ascribed to the higher separation efficiency of the new method.

Fractionation Equilibria

For the simulation of CPF experiments with PC reported in the next section, the parameters M_{seg} and ξ have to be determined as already described in the context of the evaluation of published CPF experiments with PE. Although it would be no problem to consider the mixed solvents used in the case of PC theoretically, the additional expense was avoided in view of the fact that it appears unnecessary if one is not interested in the composition of the mixed solvent in the coexisting phases. In the present simulation, the constituents of the solvent were therefore treated as one component for which the weight average molar mass was used. In the limited concentration regime of interest, M_A was taken to be constant at 88.5 g/mol. Figure 8 shows the B–W plots used for the determination of the parameters

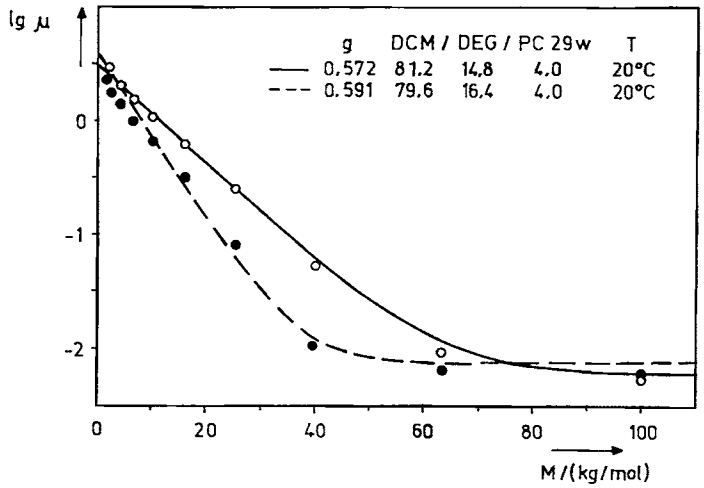

Figure 8 B–W plot for two-phase equilibria with PC under the conditions given in this graph. Points represent a selection of measured data; lines are calculated theoretically with M_{seg} = 70 g/mol (as compared with the average value M_A = 88.5 g/mol resulting from the molar masses of the components of the mixed solvent) and ξ = 0.002.

necessary to model CPF of PC theoretically; resulting data are given in the legend.

CPF Simulations

In this section, we examine to what extent the theoretical calculations can describe reality and how they can be used to obtain further insight into CPF procedures. The results of this evaluation should be helpful in the optimization of the fractionation. Such simulations can be performed regarding many aspects. Here, they are confined to the most important ones.

Determination of Theoretical Plates

Using the above parameters for the description of the phase separation behavior of the system DCM/DEG/PC, it is now possible to evaluate the results of the different CPF runs with respect to the number of theoretical plates that could be realized with the improved method. Two examples for the representation of the fractionation efficiencies in terms of B–W plots are given in Figure 9; from this graph, it can be seen how the experimentally obtained partition of the polymer homologues on the fractions are reproduced if the appropriate integer number of theoretical plates are chosen. For CPF runs C1–C4 and D (cf. Table II), values of 4 or 5 were obtained.

The results of the above evaluation can be seen in terms of the molecular weight distributions of the starting material and of the two fractions in Figure 10 for CPF run C1. It is worthwhile to note how well the theoretical calculations coincide with the actual behavior despite the simplifying assumptions made.

Approach of Stationary States

For the mastering of the process, it is also essential to reach a better theoretical understanding of the initial stages of the continuous polymer fractionation procedure. By means of the present approach, such data can be easily obtained from the results of CPF simulation before stationary states are reached, i.e., for small values of j. The comparison of these results with actual measurements is performed in Figure 11 for the first removal of sol phase from the column (experiment) or from the system (theory).

The molecular nonuniformity of the polymer in the first gel fractions is less than in the stationary state because of the larger amounts of material extracted in the sol phase during that stage. Correspondingly, U^{SL} is larger in the nonstationary than in the stationary state. To compensate for this effect at least partly, it is advisable to chose a lower temperature of the condenser during the initial state and raise the amount of polymer refluxed. With this precaution, the comparatively long time required to reach stationary states (with the present apparatus, up to 12 h) does not constitute an inconvenience.

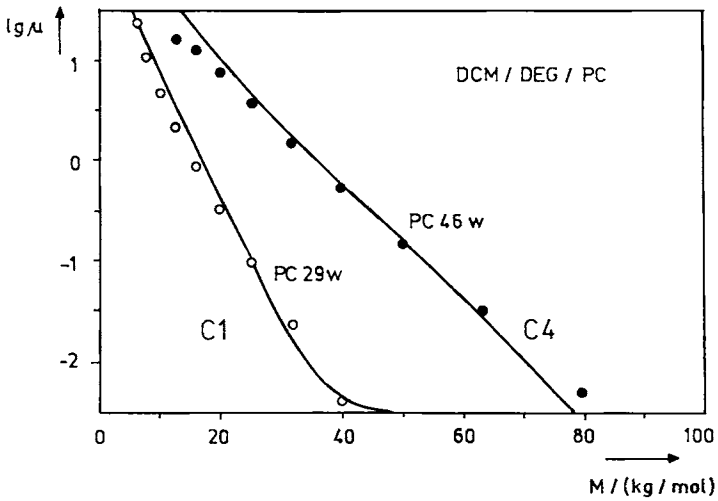

Figure 9 B–W plot for the two CPF experiments indicated in the graph. Data points were measured and lines calculated. For run C1 (Table II), the number of theoretical plates was set to 4, and for the interaction parameters $g_{column} = 0.593$ and $g_{condenser} = 0.607$, respectively), for run C4 the corresponding data read: five plates, $g_{column} = 0.554$, $g_{condenser} = 0.560$.

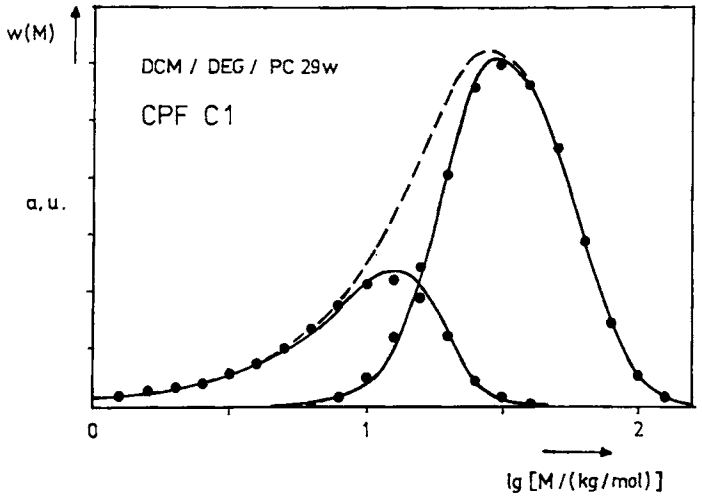

Figure 10 Differential molecular weight distribution of the polymer in the feed (dotted line) and of the sol and gel fractions, respectively, resulting from CPF run C1. Points represent experimental values and full curves give the result of the theoretical simulation for which the parameters named in Fig. 9 were used.

Predictive Power

If the thermodynamic parameters of the polymer/solvent system used for CPF are available (for instance, by phase equilibria measurements) and if the number of theoretical plates of the apparatus can realistically be estimated, it is possible to calculate how a certain desired fractionation can best be performed.

In fact, such a prediction has been performed prior to the realization of the improved CPF for two series fractionations: (1) four theoretical plates, polymer loading of 2 wt %, five equal fractions; and (2) five plates, 3 wt %, and six equal fractions. The fractionation efficiency is essentially the same in both cases since the larger number of theoretical plates and fractions of (2) is compensated by the higher polymer concentration. Variant (1) corre-

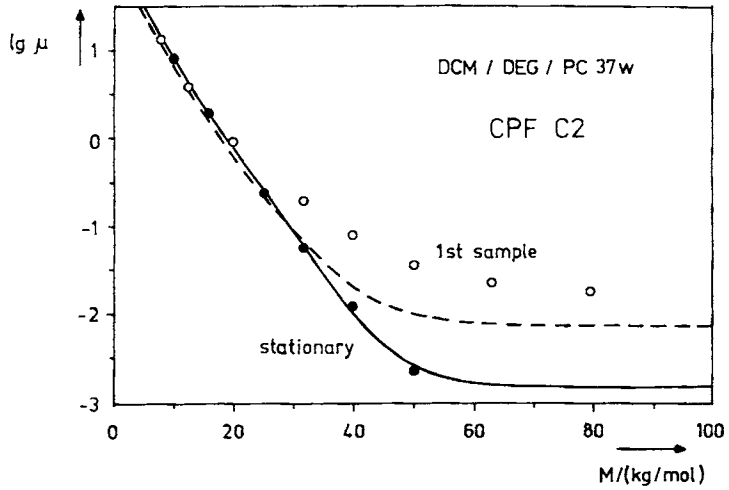

Figure 11 Comparison of fractionation achieved during stationary operation of the CPF and in its initial stage by means of B–W plots; the present example is given for run C2. The initial stage is characterized by the first removal of sol phase, the gel phase being already withdrawn before. The experimental parameters can be seen from Table II and the following data were used for the simulation: $m_{max} = 4$, $g_{column} = 0.581$, $g_{condenser} = 0.593$. Experimental results are given by full (stationary) and open (nonstationary) circles; the corresponding lines were calculated theoretically.

sponds in reasonable approximation to the actually performed experiments C1–C4.

OUTLOOK

In the present communication, it was demonstrated how considerable theoretical and experimental improvements of CPF could be achieved. It is meanwhile possible to produce practically any amount of fractions with the desired molecular uniformity by means of very simple equipment as long as solvents are available with which liquid/liquid phase equilibria can be realized. Today, CPF is primarily of importance in the field of research where good fractions are often required. It can, however, be anticipated that this method will become of practical use in the field of specialty polymers, like substances of pharmaceutical interest or photoresists. Furthermore, CPF is naturally not restricted to the separation of polymers according to their chain length. It can also be applied to macromolecules, which differ in their solubility for other reasons, for instance, as a result of their different content of comonomers. It is self-evident that CPF has to be optimized for each special application; by means of the presented theoretical approach this should, however, not be a major problem.

NOMENCLATURE

G	segment-molar Gibbs energy
g	(integral) interaction parameter [eq. (14)]
$K(r)$	degree of precipitation [eq. (7)]
M	molar mass (molecular weight)
M_w	weight average molecular weight
p	concentration parameter of g [eq. (15)]
r	number of segments [eq. (1)]
U	molecular nonuniformity [$U = (M_w/M_n) - 1$]
w	weight fraction
$w(r)$	extensive segment-molar distribution function
$W(r)$	intensive segment-molar distribution function
ξ	adjustable parameter [eq. (20)]
μ	$w'(M)/w''(M)$
Φ	relative amount of segments of phase $''$
Ψ	overall segment fraction of all polymer species

Subscripts

A	solvent
FD	feed phase of the CPF
seg	segment
j	step j of calculation
m	theoretical plate m of the column

Superscripts

$'$	less concentrated coexisting phase
$''$	more concentrated coexisting phase

REFERENCES

1. H. Geerissen, J. Roos, and B. A. Wolf, *Makromol. Chem.*, **186,** 735 (1985).
2. H. Geerissen, J. Roos, P. Schützeichel, and B. A. Wolf, *J. Appl. Polym. Sci.*, **34,** 271, 287 (1987).
3. H. Geerissen, P. Schützeichel, and B. A. Wolf, *Makromol. Chem.*, **191,** 659 (1990).
4. R. Koningsveld, L. Kleintjens, H. Geerissen, P. Schützeichel, and B. A. Wolf, in *Comprehensive Polymer Science,* G. Allen, ed., Pergamon Press, Oxford, UK, 1989, p. 239.
5. M. T. Rätzsch, L. Tschersich, and H. Kehlen, *J. Macromol. Sci.-Chem. A* **27,** 999 (1990).
6. H. Kehlen and M. T. Rätzsch, *Z. Phys. Chem. (Leipzig),* **264,** 1153 (1983).
7. M. T. Rätzsch and H. Kehlen, *J. Macromol. Sci.-Chem. A,* **22,** 323 (1985).
8. M. T. Rätzsch, H. Kehlen, and L. Tschersich, *J. Macromol. Sci.-Chem. A,* **26,** 921 (1989).
9. J. W. Breitenbach and B. A. Wolf, *Makromol. Chem.,* **108,** 263 (1967).
10. G. Glöckner, in *Polymerfraktionierung durch Flüssigkeitschromatographie* 1st ed., Hüthig-Verlag, Heidelberg, 1982, p. 134 ff.

Received March 21, 1991
Accepted August 22, 1991